Nuclear Instruments and Methods in Physics Research B 550 (2024) 165319

Contents lists available at ScienceDirect

Nuclear Inst. and Methods in Physics Research, B

journal homepage: www.elsevier.com/locate/nimb

Comparing the effect between room temperature and low temperature heavy ion irradiation by deep level transient spectroscopy

Xu Gao [a], Xuanyu Wang [a], Yun Li [a,b], Zhimei Yang [a,b,*], Min Gong [a,b], Mingmin Huang [a,b], Yao Ma [a,b]

[a] Key Laboratory for Microelectronics, College of Physics, Sichuan University, Chengdu 610065, China
[b] Key Laboratory of Radiation Physics and Technology of Ministry of Education, Sichuan University, Chengdu 610065, China

ARTICLE INFO

Keywords:
4H-Silicon carbide
Heavy ion irradiation
Low temperature irradiation
Room temperature irradiation
Deep level defect

ABSTRACT

To promote the application of SiC devices in extreme environments, the irradiation damages of 4H-SiC Schottky barrier diodes (SBDs) irradiated with 6 MeV Au ions under room temperature (RT) and low temperature (LT) were investigated in this work. Deep level transient spectroscopy (DLTS) was used to analyze the changes in primary defects. DLTS measurements indicated the presence of six deep levels labeled EN, E_1, E_2, E_3, E_4 and E_5. Notably, the peak positions for the samples irradiated under RT shifted to the right compared to those irradiated at LT with increasing fluence. This means that the deeper energy defects are produced under RT irradiation. The experimental results also demonstrated that the HI irradiation-induced defects are mainly located at interface between metal and SiC, especially the metal–semiconductor (M−S) interface edge. Therefore, these results suggest that the evolution of defects in SiC devices under LT and RT irradiation,which is helpful to provide its application in power electronics and extreme environments.

1. Introduction

Silicon carbon (SiC) with a wide bandgap, high thermal conductivity, and other excellent material characteristics can better work in high temperature, high power, high frequency [1–3], rich irradiation environmental conditions [4,5] than silicon, so it is widely used in aerospace, military, photovoltaic and other fields. Intrinsic defects in SiC have attracted extensive attention due to the prospect of its components of quantum technology [6]. At present, there are numerous studies on the irradiation effects of proton[7], neutron[8], electron [9] and heavy ion (HI) [10] on SiC devices.

Based on the principle of deep level transient spectroscopy (DLTS), the correlation parameters of impurities, defects and interface states in the band gap range can be obtained by scanning the temperature. As a result, DLTS was a technique used to analyze the correlation parameters of the irradiation-induced defects of SiC Schottky barrier diodes (SBDs) [11–13]. These results suggest that irradiation-induced defects can lead to a decrease in the height of the Schottky barrier and an increase in reverse leakage current, which can affect the electrical performance of SiC SBDs [14]. In particular, the displacement damage is the most prevalent among the ion irradiation effects, which can impact the lattice integrity of semiconductor materials and produce interstitial atoms or vacancy defects. In severe cases, the carrier mobility may reduce and the carrier compensation effect will also occurs, which can further affect the electrical or optical properties of the SiC material and device. Previous studies have shown that there are many defects in 4H-SiC [15], including E_1, Z_1/Z_2, $RD_{1/2}$, EH_6/EH_7, etc. E_1 is related to the carbon interstitial(C_i) [16–18]. Z_1/Z_2 is associated with carbon vacancies(V_C) in which diffuse suspension bonds (negative U centers) exist [19–21]. $RD_{1/2}$ is associated with positively charged silicon vacancies(V_{Si}) [22,23]. The higher order clusters of EH_6/EH_7 are also V_C. For the aforementioned applications, understanding the irradiation-induced defects in SiC, particularly their evolution under different temperature conditions, is crucial for applications in power electronics in extreme environments. With the development of space exploration technology and deep space technology, the power electronics often operate under low temperature (LT) conditions. It has been observed that the thermal emission model was not appropriate for LT, and the generation-recombination was dominant [14], which leads to a decrease in the turn-on voltage (V_{ON}). While the LT irradiation effects on 4H-SiC devices have received relatively less attention compared to other materials like GaN and GaAs [24–27], our latest findings show that joule heating causes a short-time

* Corresponding author at: Key Laboratory for Microelectronics, College of Physics, Sichuan University, Chengdu 610065, China.
E-mail address: yangzhimei@scu.edu.cn (Z. Yang).

https://doi.org/10.1016/j.nimb.2024.165319
Received 6 June 2023; Received in revised form 5 March 2024; Accepted 7 March 2024
Available online 15 March 2024

annealing effect during swift heavy ion irradiation (SHI), which can cause the partial damage or defects to be recovered [10]. Therefore, in order to avoid the recrystallization effect observed with RT SHI irradiation, the LT irradiation is carried out in this work. Meanwhile, the main goal of this work is also to analyze the different irradiation mechanisms for defects induced by LT and RT irradiation, with the aim of improving the application of 4H-SiC power devices in extreme conditions. Furthermore, the evolution of the defects under RT and LT HI irradiation on commercial 4H-SiC SBDs is investigated by DLTS.

2. Experimental detail

In this study, the electronic characteristics of a commercial 4H-SiC SBDs were measured, which are fabricated by Cree Inc. (CSD01060, 600 V, 10 A, the active areas estimated to be 0.5 mm^2). The SiC SBD has an Al/W/WTi/Ti metal layer, where the thickness of W/WTi/Ti is 135 nm, 212 nm, and 98 nm, respectively [14].

The irradiation portion of the experiment was carried out at the 3 MeV Tandtron accelerator at the Institute of Nuclear Science and Engineering of Sichuan University. 30.46 keV/U^{197} Au^{2+} ion beam was perpendicular to device under test (DUT), the irradiation environment temperatures were 77 K(LT) and 300 K(RT), respectively. The beam flux comes from the rastering beam. The irradiation fluences were selected to be 1×10^{13} ions/cm^2, 1×10^{14} ions/cm^2, 1×10^{15} ions/cm^2, and 5×10^{15} ions/cm^2, respectively. The irradiation rate was 5×10^{12} ions/(cm^2·s). Fig. 1 illustrates the schematic representation of the metal structures and layout of heavy ion (HI) irradiation on the 4H-SiC SBD. It can be observed that the whole epitaxial layer is not completely covered by the metal electrode, but the entire surface of the 4H-SiC SBD undergoes irradiation.

To monitor the temperature during the irradiation, a FLIR thermal imaging camera (A655sc) was used. The camera captured thermal images at a resolution of 640 × 480 pixels and a frame rate of 50 frames per second, and the accuracy is approximate ± 2 °C. Fig. 2 shows the detection of the actual ambient temperature of the sample under the fluences of 5×10^{15} ions/cm^2 under RT(Fig. 2 (a)) and LT(Fig. 2 (b))

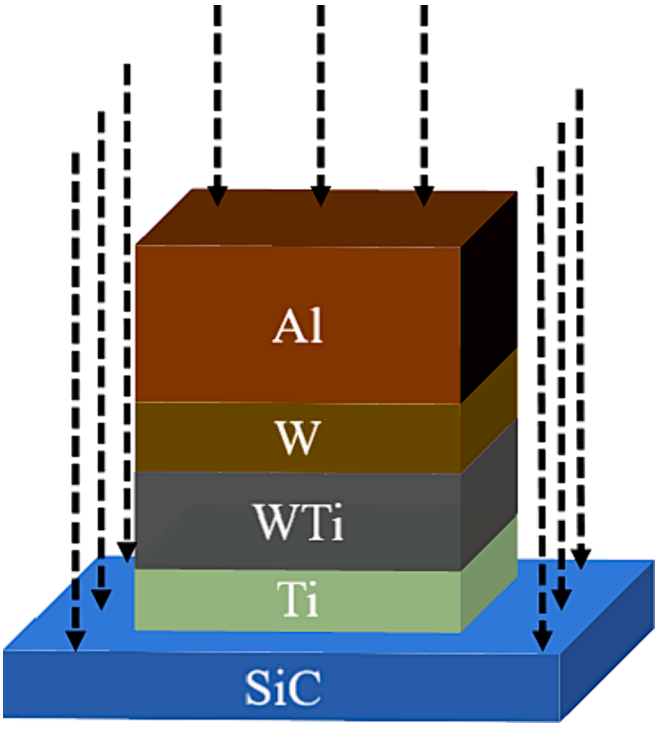

Fig. 1. The schematic of the metal structures and irradiation layout of 4H-SiC SBD.

irradiation. According to the Fig. 2 (a), the highest temperature reaches 240 ℃ under RT irradiation, with temperatures at S1 and S2 recorded as approximately 195.8 ℃ and 163.8 ℃.Under LT irradiation, the highest ambient temperature reached 120 ℃ (Fig. 2 (b)), with temperatures at S1 and S2 recorded as approximately 50.6 ℃ and 51.9 ℃.

The irradiation induced defects were measured by FT1230 Deep Level Transient Spectroscopy of Germany PhysTech. Only one temperature scan is needed for 28 tempscans and 28 Arrhenius plot points for one measurement parameter set. Therefore, the temperature scanning was performed from 40 K to 500 K, and the reverse bias(U_R) was set to −1, −2, −4 and −6 V, respectively, to observe the changes of the defects. Then the other test conditions were selected as follows: T_W is measurement period width, T_P is filling pulse width, U_P is filling pulse.TW = 100 ms, T_P = 100 μs, and U_P = -0.2 V.

3. Experimental results and discussion

In order to better investigate the damage of HI irradiation on 4H-SiC SBD devices, the changes in the irradiation-induced deep level defects under LT and RT HI irradiation are observed by DLTS. Fig. 3 (a) and (b) show the DLTS for the sample irradiated with a fluence of 1×10^{15} ions/cm^2 under RT and LT irradiation, respectively. For the sample with 1×10^{15} ions/cm^2 by RT irradiation in Fig. 3 (a), it can be found that there are four defect peaks labeled EN, E_3, E_4 and E_5, respectively. The intensity of the negative EN signal increases with increasing U_R, while the remaining three peaks reach their maximum and shift to the right at −2 V, then the position of E_5 keeps unchanged with increasing U_R. Similarly, four defect peaks labeled EN, E_2, E_4 and E_5 are observed for the sample with 1×10^{15} ions/cm^2 by LT irradiation (Fig. 3 (b)). The intensity of EN, E_2, E_4 DLTS signal also increases with the increase of U_R. The E_5 signal reaches its maximum and shifts to the right at −2 V, then intensity of E_5 decreases and the position of E_5 remains unchanged with increasing U_R.

To determine the energy level position and capture cross-section of the defects observed, the formula (1) can be used.

$$ln\left(\frac{e_n}{T^2}\right) = ln(K\sigma_n) - (E_c - E_T)/kT \quad (1)$$

σ_n is the capture cross section, E_C-E_T is the energy level position, K is a constant related to the capture cross section and effective mass and independent of temperature, e_n is the emission rate, k is the Boltzmann constant. According to formula (1), we can calculate the energy level position and capture cross section of the corresponding defect energy level by the slope and intercept of the curve in Fig. 5.

According to the principles of the semiconductor physics, the width of depletion region is estimated to be approximately 0.69 μm, 0.83 μm, 0.95 μm, 1.3 μm at reverse biases of −1 V, −2 V, −4 V and −6 V, respectively. Consequently, the increase in width of the depletion region increases with the application of reverse bias by the principle of the DLTS test, and the DLTS results correspond to the different depletion layers under the same U_p and the different U_R. From Fig. 3 (a) and (b), it can be observed that the DLTS peak is the highest at −2 V for both samples. This indicates that the E_4 and E_5 defects, which reach their maximum intensity, are located near the surface of the SiC epitaxial layer. The local amplification diagram in the inset of Fig. 3(a) depicts the impact of Au ion incidence at the metal edge. It can be observed that the irradiation can not only affect the region covered by the metal, but also influence the terminal region without metal layers. Based on the research utilizing the stopping and range of ions in matter (SRIM), Au ions are unable to penetrate the metal layer in region covered by metal, but the vertical range of Au ions in the epitaxial layer can reach depths of 1.7 μm vertically and 1.1 μm horizontally in the region without metal layer, respectively. Hence the metal layer can effectively block the majority of Au ions penetrating into 4H-SiC epitaxial layer, but secondary particles, such as electrons, have the potential to impact the

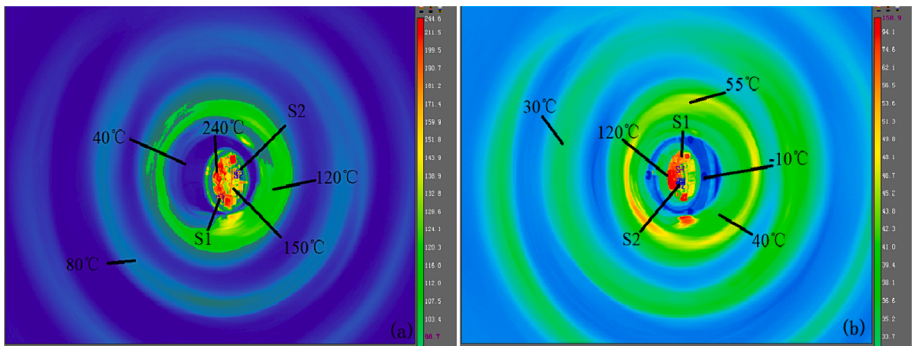

Fig. 2. Actual ambient temperature under (a) RT irradiation and (b) LT irradiation.

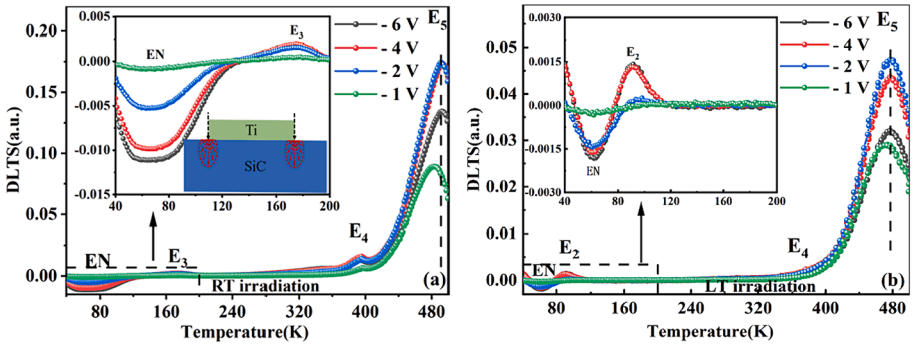

Fig. 3. DLTS spectra of different reverse bias of the samples irradiated by 1×10^{15} ions/cm^2 (a) under RT irradiation and (b) under LT irradiation.

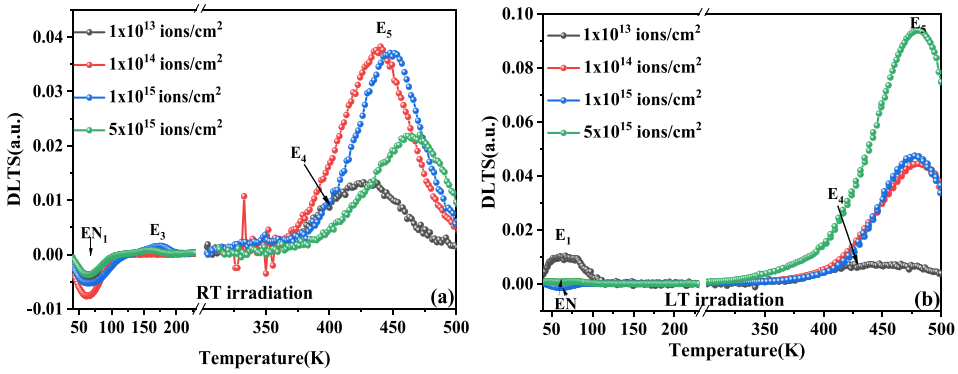

Fig. 4. DLTS spectra of samples under (a) RT irradiation and (b) LT irradiation.

metal–semiconductor (M−S) interface, especially near the terminal region without metal layers. HI irradiation induces defects and defect states in the epitaxial layer, and futher lead to the deterioration of the M−S interface near the terminal region without metal layers. Therefore, the M−S interface edge is a critical region for the electrical characteristics of SBD devices and also the most sensitive area to irradiation. The E_5 center with large σ_n, acts as an efficient recombination center for the sample with 1×10^{15} ions/cm^2 under RT irradiation. Additionally, as can be seen in the Fig. 3, for the sample with 1×10^{15} ions/cm^2, it is noted that the peak of E_5 shows a rightward shift of −2 V then keeps unchanged with increasing U_R both RT irradiation and LT irradiation. Interestingly, the ionization peak position moves to the right, while the displacement peak position remains unchanged with increasing reverse bias. This suggests that E_5 represents a broad energy level encompassing both ionization defects and displacement defects. When Au^{2+} ions interact with the device, the small amount of Au ions and secondary particles predominantly impact the width of the depletion layer corresponding to U_R = -2 V(0.83 μm). This exceeds the concentration of displacement defects present in the material, thereby emphasizing the prevalence of the ionization effect. Nevertheless, in the deeper positions of the depletion layer, the influence of Au ions and secondary particles is minimal, primarily contributing to the displacement effect. As a result, the peak E_5 remains unchanged in these regions. These observations align with the finding that the defects are primarily concentrated at the interface position. The variation in the peak value of displacement defect is attributed to the interaction between ionization and displacement defects, while the change in peak value of the ionization defect is influenced by the electrostatic field effect. When the reverse bias exceeds −2 V, the DLTS peak value decreases instead. This behavior can be explained by the reduction in the capacitance of the depletion region, which is inversely related to the applied reverse bias according to the equation (2).

$$C_0 = A\sqrt{\frac{\varepsilon_0 \varepsilon_{4H-SiC} q N_D}{2(V_R + V_D)}} \tag{2}$$

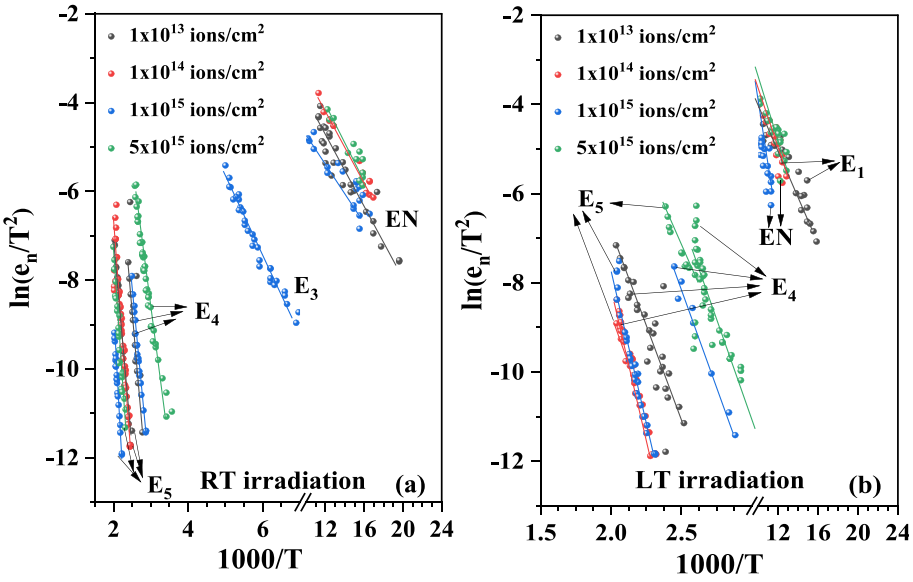

Fig. 5. Arrhenius curves under (a) RT irradiation and (b) LT irradiation.

where A is the area of the SBD, V_D is the built in potential, N_D is the effective doping concentration, ε_0 is the permittivity of free space,ε_{4H-SiC} is the permittivity of 4H-SiC, q is the elementary charge, and V_R is the applying reverse bias.

If $N_T \ll N_D$, the trap center is completely filled with free electronics

$$\Delta C_0 = A\sqrt{\frac{\varepsilon_0\varepsilon_S q(N_D - N_T)}{2(V_R + V_D)}} - A\sqrt{\frac{\varepsilon_0\varepsilon_S q N_D}{2(V_R + V_D)}} \approx -C_0\frac{N_T}{2N_D} \quad (3)$$

In equation (3), it is important to note that the N_T reaches its maximum at −2 V. This means that the trap defects are mainly distributed within a range of 0.83 μm. Hence only these trap defects make a contribution to the minority trap capacitance transient. The decrease in capacitance of the depletion region is attributed to the capture of the electrons by the majority carrier traps. As a result, the absolute value of ΔC_0 decreases. Consequently, the DLTS peak value also decreases. Additionally, the results also indicate that the ionization defect peak position shifts to the right with the increase in reverse bias, while the displacement peak position remains unchanged (Table 1).

For the characterization of irradiation-induced deep level defects in 4H-SiC SBDs, DLTS measurements were performed with $T_W = 100$ ms, $T_P = 100$ μs, $U_P = -0.2$ V and $U_R = -2$ V, as shown in Fig. 4. According to the Fig. 4 (a), the DLTS spectrum for the samples by RT irradiation reveals four traps labeled EN, E_3, E_4 and E_5. Their energy levels and electron σ_n can be determined from the Arrhenius plot,as summarized in Table 2. Among these, the E_5 trap dominates over the entire temperature scan range. The negative peak (labeled EN) may be related to the implantation process in SiC device technology. Commercial devices often include termination and guard rings made by p-doping [28], therefore, the EN peak may come from the majority carrier trap in these p-type layers. It is observed that the intensity of the DLTS spectrum reaches the maximum under RT irradiation with 1×10^{14} ions/cm^2 and then decreases. Meanwhile, the DLTS spectrum of the sample under RT

Table 2
Extracted DTLS parameters for all detected trap types from this work.

Samples	Fluence(ions/cm^2)	Level	E_C-E_T(eV)	σ(cm^2)	N_T(cm^{-3})
RT Irradiation	1×10^{13}	EN	0.04	$<10^{-18}$	8.9×10^{12}
		E_4	0.75	1.1×10^{-16}	1.0×10^{12}
		E_5	0.95	1.3×10^{-15}	7.6×10^{13}
	1×10^{14}	EN	0.03	$<10^{-18}$	1.3×10^{13}
		E_5	0.90	4×10^{-16}	1.1×10^{14}
	5×10^{15}	EN	0.03	$<10^{-18}$	1.0×10^{13}
		E_4	0.60	3.8×10^{-17}	4.6×10^{12}
		E_5	0.99	1.4×10^{-15}	2.7×10^{12}
LT irradiation	1×10^{13}	E_1	0.04	$<10^{-18}$	1.4×10^{13}
		E_4	0.70	3.1×10^{-18}	6.8×10^{12}
	1×10^{14}	E_1	0.03	$<10^{-18}$	7.1×10^{12}
		E_4	0.72	1.1×10^{-16}	2.4×10^{12}
		E_5	1.07	6×10^{-15}	3.7×10^{13}
	5×10^{15}	EN	0.04	$<10^{-18}$	1.7×10^{13}
		E_4	0.65	5.1×10^{-17}	1.6×10^{13}
		E_5	1.17	2×10^{-13}	1×10^{14}

Table 1
Provides E_C-E_T, σ_n, trap concentrations (N_T), and other relevant information for the traps observed in the 4H-SiC SBDs with a fluence of 1×10^{15} ions/cm^2 under RT and LT irradiation.

Samples	Level	E_C-E_T (eV)	σ_n (cm^2)	N_T (cm^{-3})	Possible defects
RT irradiation	EN	0.03	$<10^{-18}$	1.7×10^{13}	p-doping [28]
	E_3	0.15	$<10^{-18}$	2.8×10^{12}	Ti_{Si}(k) [22]
	E_4	0.77	5.0×10^{-16}	1.25×10^{13}	Z_1/Z_2(C/Si vacancy) [20]
	E_5	1.12	6.2×10^{-15}	1.6×10^{14}	C clusters [7,16]
LT irradiation	EN	0.06	$<10^{-18}$	1.2×10^{13}	p-doping [28]
	E_2	0.10	$<10^{-18}$	1.2×10^{13}	Ti_{Si}(h) [22]
	E_4	0.65	1.6×10^{-17}	1.1×10^{12}	Z_1/Z_2(C/Si vacancy) [20]
	E_5	1.26	7.7×10^{-13}	5×10^{13}	C clusters [7,16]

irradiation shifts to the right with increasing fluence. Noted that there are three obvious peaks labeled EN, E_4 and E_5 for the samples by LT irradiation from the Fig. 4 (b), while the maximum value of the intensity occurs at 5×10^{15} ions/cm^2 under LT irradiation. It is also worth mentioning that the DLTS spectrum with the fluence of 1×10^{13} ions/cm^2 exhibits a broad peak in the temperature range of 400–500 K, indicating that it is formed by the overlapping of several closely position peaks.

The Arrhenius plot, extracted and calculated from Fig. 3 (a) and (b), is shown in Fig. 5 to obtain further information about the defect energy level. From the Fig. 5, it is shown that the peak E_1 is located at approximately E_C-0.04 eV, the peak E_4 is around E_C-0.70 eV, and the E_5 energy level is approximately E_C-1.0 eV. The parameters of the defect energy level are calculated and summarized in Table 2, which can provide valuable information regarding the characteristics of these defect energy levels.

In order to more clearly observe the variation in peak height of the defects dependent on the irradiation fluence, the change of peak height with the fluence is plotted in Fig. 6 (a) and (b). It can be observed that two new energy levels appear when the fluence exceeds 1×10^{15} ions/cm^2 under RT, and the peak height of the defect does not increase as the fluence increases. Under LT irradiation, the peak height of E_1 is too weak to be shown in the Fig. 6 (b). However, the peaks corresponding to E_4 and E_5 increase with the increase of fluence except for the fluence at 1×10^{13} ions/cm^2. According to the DLTS spectrum, the energy level concentration increases with the increasing peak height, and the depth of the energy level position is correlated with the x-axis coordinate of the peak position. From the Table 2 and Fig. 6, it can be observed that there are significant differences in the parameters of the defect energy levels under different irradiation conditions, although they belong to the same energy level type.

The main defects observed in 4H-SiC and 6H-SiC are illustrated in the Fig. 7. For 4H-SiC, the energy level EH_1 (E_C-0.31 eV) [7,9,12,29,30] is attributed to the presence of carbon interstitial (C_i), the Z_1/Z_2 (E_C-0.68 eV) [9,10,12,31] is associated with the carbon vacancy at the hexagonal (V_C(h)) and pseudocubic site (V_C(k)) of the lattice, and the energy level $RD_{1/2}$ (E_C-0.88 eV) [31] is generated by the positively charged V_{Si}. In recent years, the Z_1/Z_2 center has been identified as a major carrier lifetime killer in n-type 4H-SiC [32,33]. Therefore, it is really significant to reduce and control the concentration of Z_1/Z_2, and two employed techniques include introducing excess carbon atoms from the external sources and promoting the diffusion of these carbon atoms into the bulk region through high-temperature annealing [34,35], as well as the thermal oxidation of SiC under appropriate conditions to eliminate the $Z_{1/2}$ center [36]. When it comes to the change in the concentration of V_C and V_{Si}, new defects may be generated. For example, EH_5 (E_C-1.15 eV) [12,29,31] is associated with carbon vacancy silicon antisites (V_C-C_{Si}), while $EH_{6/7}$ (E_C-1.50 eV) [37] is assigned to the donor state of the V_C. In addition, DLTS also observes some impurity levels, such as the N impurity energy level (E_C-0.06 eV) [7,9,29,38] resulting from the intentional doping of nitrogen in the SiC process, and the Ti impurity energy level with E_C-0.11 eV and E_C-0.15 eV [7,9,29,30,38] originating from the hexagonal Ti_{Si}(h) and pseudocubic Ti_{Si}(k) sites in the lattice. The presence of the energy level SF (Ec-0.23 eV) [30] observed in HI irradiation is considered to be a single common stacking fault. For 6H-SiC, the main defects include the E_1/E_2 [12,39–42] energy level with E_C-0.36 eV and E_C-0.44 eV formed by the V_C(h) and V_C(k), the E_i [40–43] energy level with E_C-0.50 eV closely related to the V_C, the Z_1/Z_2 [12,39–43] energy levels with E_C-0.62 eV and E_C-0.68 eV originated from the silicon vacancies(V_{Si}), and R [12,39] center with E_C-1.25 eV linked to high-order V_C. Previous studies have reported that proposed that the Z_1/Z_2 and EH_7 energy levels in 4H-SiC correspond to the E_1/E_2 and R centers in 6H-SiC by systematic DLTS investigations [12], respectively. Additionally, according to the latest research [44], there can be coupling effect when multiple defect levels act simultaneously in semiconductor materials, enabling the direct and effective charge transfer between two energy levels. At specific energy level, the charge transfer between defects can enhance carrier recombination and lead to more severe damage.

According to the results presented in the previous section, it can be observed that the peak E_1 exhibits similarities to the N impurity energy level shown in Fig. 7, with similar activation energy and σ_n under LT HI irradiation. For the samples irradiated under RT and LT irradiation, two notable differences can be identified. The first distinction is between the peaks of E_2 and E_3. The E_2 energy level observed under LT irradiation can be attributed to the ionized Ti_{Si}(h), but the E_3 energy level observed after RT irradiation corresponds to the Ti_{Si}(k), which has a deeper energy defect level compared to Ti_{Si}(h). This difference may be due to the fact that the system temperature during RT irradiation is higher compared to the cryogenic irradiation, resulting in formation of deeper energy defect under RT irradiation. In addition, the appearance of the E_2 and E_3 for the fluence greater than 1×10^{15} ions/cm^2 suggests that the formation is related to the fluence. However, these peaks disappear when the irradiation fluence reaches 5×10^{15} ions/cm^2, indicating the irradiation fluence exceeded the threshold range that the material can withstand, and the impurity compensation phenomenon manifests. Therefore, the Ti_{Si}(h) defect is likely located near the interface between metal layer and SiC, which can greatly affect the Schottky barrier height of the devices. The second difference arises in the peak E_5, which exhibits similarities to the EH_5 defect energy level shown in Fig. 7, and is related to carbon clusters. The peak position of E_5 shifts to the right with the increase of fluence under RT irradiation, indicating that the energy level position became deeper with the increase of fluence. On the other hand, the peak positions of E_5 peaks with different fluences remain relatively unchanged under LT irradiation, which means the energy level positions are consistent. Furthermore, under LT irradiation, the DLTS intensity of E_5 increases with the increasing fluence, while the behavior is different under RT irradiation, and the peak E_5 reaches its

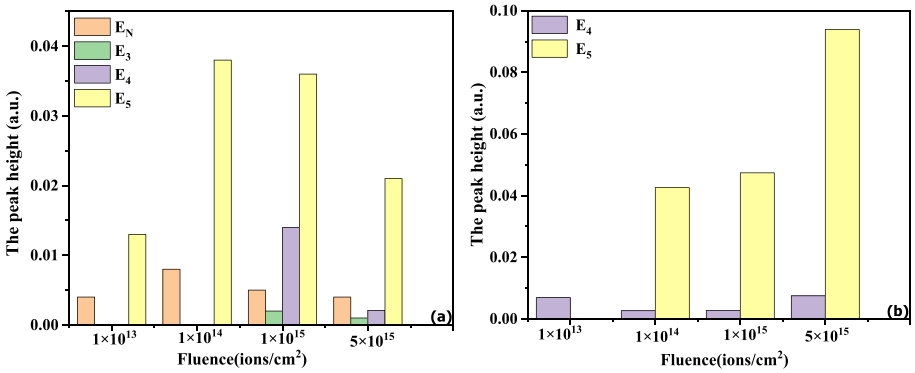

Fig. 6. Changes in the peak height of the defects with the fluence under (a) RT irradiation and (b) LT irradiation.

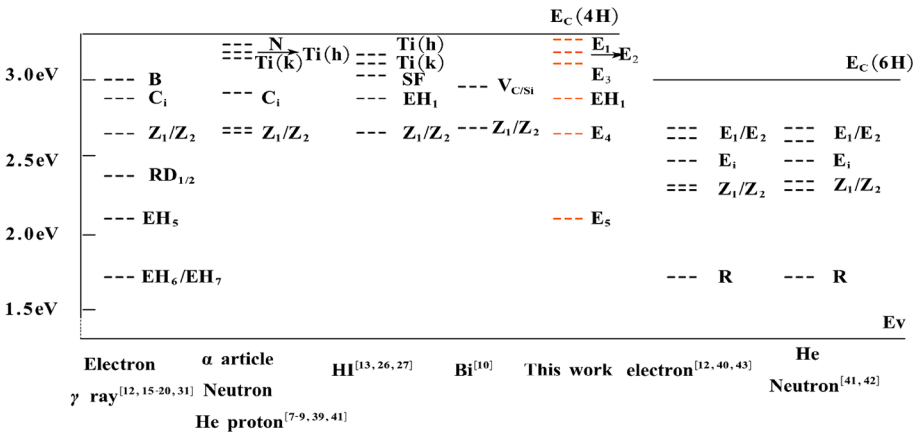

Fig. 7. Defect energy level diagram of 4H-SiC and n-6H-SiC

maximum intensity at 1×10^{14} ions/cm^2. The difference between RT and LT irradiation could be explained by the higher ambient temperature during RT irradiation, as shown in Fig. 2. Although there is some heat dissipation in the environment, the lattice vibrations caused by energy exchange during irradiation are still significant, which makes the concentration of unstable defects decrease and the interface trap effective level gradually shift towards the bottom of the band gap, finally resulting in a right shift of the peak position. Therefore, the partial defect recovery occurs, and the peak height also decreases accordingly. In addition, the peak E_4 corresponds to the Z_1/Z_2 center in Fig. 7, which is formed by the V_C. The peak E_4 may not be clearly visible in the DLTS spectrum at fluence of 1×10^{14} ions/cm^2 under RT irradiation, as it may be included within the peak E_5.

4. Conclusion

In this work, the irradiation damage of SiC SBD caused by RT and LT HI irradiation is investigated. After 6 MeV Au ions irradiation, the DLTS spectrum revealed the presence of EN(p-doping), $E_1(N_{hs})$, $E_2(Ti_{Si}(h))$, $E_3(Ti_{Si}(k))$, $E_4(Z_1/Z_2$(C vacancy$_i$)), $E_5(V_C$-$C_{Si})$ defects. The defect energy level primarily resides near the surface in close proximity to the SiC epitaxial layer, particularly near the terminal region without metal layers. Comparing the results between the two irradiation conditions, the sample irradiated with a fluence of 1×10^{14} ions/cm^2 under RT irradiation shows the highest peak, but the DLTS intensity of the sample with 5×10^{15} ions/cm^2 is the largest. This implies that a significant amount of heat is generated during RT irradiation, which can lead to the recrystallization effect in SiC semiconductors. Furthermore, the annealing effects are more pronounced during RT irradiation compared to LT irradiation, resulting in a decrease in peak height and a rightward shift of the peaks with increasing irradiation fluence.

CRediT authorship contribution statement

Xu Gao: Writing – original draft, Visualization, Investigation, Formal analysis, Data curation, Conceptualization. **Xuanyu Wang:** Investigation, Formal analysis, Data curation. **Yun Li:** Project administration, Methodology. **Zhimei Yang:** Writing – review & editing, Supervision, Funding acquisition. **Min Gong:** Writing – review & editing, Supervision. **Mingmin Huang:** Writing – review & editing. **Yao Ma:** Writing – review & editing, Resources.

Declaration of competing interest

The authors declare that they have no known competing financial interests or personal relationships that could have appeared to influence the work reported in this paper.

Data availability

Data will be made available on request.

Acknowledgments

This project is supported by the National Natural Science Foundation of China under Grant No. 61704116, Natural Science Foundation of Sichuan Province under Grant No.2022NSFSC0874, Science and Technology on Analog Integrated Circuit Laboratory under Grant No. 6142802190505, and the fund of Innovation Center of Radiation Application under Grant No. KFZC2020021001.

References

[1] J. Vobecky, P. Hazdra, S. Popelka, R. Sharma, Impact of electron irradiation on the ON-state Characteristics of a 4H-SiC JBS Diode[J], IEEE Trans. Electron Devices 62 (6) (2015) 1964–1969.
[2] T. Kimoto, High-voltage SiC power devices for improved energy efficiency, Proc. Jpn. Acad., Ser. B 98 (4) (2022) 161–189.
[3] J. Grant, W. Cunningham, A. Blue, V. O'Shea, J. Vaitkus, E. Gaubas, M. Rahman, Wide bandgap semiconductor detectors for harsh radiation environments, Nucl. Instrum. Methods Phys. Res. A 546 (1) (2005) 213–217.
[4] A.Siddiqui, A. Hallén, M. Usman, Proton Irradiation-Induced Displacement Damage in 650 V Si and SiC Power Diodes. Phys. Status Solidi A 220 (21), Article 2300300(2023).
[5] F. Nava, G. Bertuccio, A. Cavallini, E. Vittone, Silicon carbide and its use as a radiation detector material. Meas. Sci. Technol. 19 (10), 102001-102001 (25) (2008).
[6] J. Coutinho, Theory of the thermal stability of silicon vacancies and interstitials in 4H-SiC, Crystals (basel) 11 (2) (2021) 1–19.
[7] E. Omotoso, A. Paradzah, P. Janse van Rensburg, M. Legodi, F. Auret, E. Igumbor, W. Meyer, Electrical characterisation of deep level defects created by bombarding the n-type 4H-SiC with 1.8 MeV protons, Surf. Coat. Technol. 355 (2018) 2–6.
[8] T. Brodar, I. Capan, V. Radulović, L. Snoj, J. Coutinho, T. Ohshima, Laplace DLTS study of deep defects created in neutron-irradiated n-type 4H-SiC, Nucl. Instrum. Methods Phys. Res. B 437 (2018) 27–31.
[9] E. Omotoso, W. Meyer, F. Auret, A. Paradzah, M. Diale, S. Coelho, P. Ngoepe, Effects of 5.4 MeV alpha-particle irradiation on the electrical properties of nickel schottky diodes on 4H-SiC, Nucl. Instrum. Methods Phys. Res. B 365 (2015) 264–268.
[10] Z.M. Yang, Y. Ma, M. Gong, Y. Li, M.M. Huang, B. Gao, X. Zhao, Recrystallization effects of swift heavy 209Bi ions irradiation on electrical degradation in 4H-SiC schottky barrier diode, Nucl. Instrum. Methods Phys. Res. B 401 (2017) 51–55.
[11] Y. Tian, R. Li, J. Li, H. Li, X. Zheng, Z. Cheng, Effects of electric polarization and defect energy levels induced by ion irradiation on the electrical behavior of 4H-SiC Schottky barrier diodes. J. Phys. D, Appl. Phys. 56(35), 355110 (2023).
[12] S. Sasaki, K. Kawahara, G. Feng, G. Alfieri, T. Kimoto, Major deep levels with the same microstructures observed in N-type 4H-SiC and 6H-SiC, J. Appl. Phys. 109 (1) (2011), 013705–13705-6.
[13] Z.M. Yang, F. Lan, Y. Li, M. Gong, M.M. Huang, B. Gao, J.K. Hu, Y. Ma, The effect of the Interfacial states by swift heavy ion induced atomic migration in 4H-SiC schottky Barrier diodes, Nucl. Instrum. Methods Phys. Res. B 436 (2018) 244–248.
[14] D.W. Wang, R.B. Hu, G. Chen, C.Q. Tang, Y. Ma, M. Gong, Q.K. Yu, S. Cao, Y. Li, M. M. Huang, Z.M. Yang, Heavy ion radiation and temperature effects on SiC schottky Barrier diode, Nucl. Instrum. Methods Phys. Res. B 491 (2021) 52–58.

[15] P. Hazdra, J. Vobecký, Radiation defects created in N-type 4H-SiC by electron irradiation in the energy range of 1–10 MeV, Phys Stat Sol. a. 216 (17) (2019), 1900312-N/a.
[16] A. Castaldini, A. Cavallini, L. Rigutti, F. Nava, Low temperature annealing of electron irradiation induced defects in 4H-SiC, Appl. Phys. Lett. 85 (17) (2004) 3780–3782.
[17] L. Storasta, J. Bergman, E. Janzen, A. Henry, J. Lu, Deep levels created by low energy electron irradiation in 4H-SiC, J. Appl. Phys. 96 (9) (2004) 4909–4915.
[18] C. Hemmingsson, N. Son, O. Kordina, J. Bergman, E. Janzén, J. Lindström, N. Nordell, Deep level defects in electron-irradiated 4H SiC epitaxial layers, J. Appl. Phys. 81 (9) (1997) 6155–6159.
[19] G. Alfieri, E. Monakhov, B. Svensson, A. Hallén, Defect energy levels in hydrogen-implanted and electron-irradiated n -type 4H silicon carbide, J. Appl. Phys. 98 (11) (2005), 113524–113524-6.
[20] Y. Wang, M. Xiang, Y. Ma, Comparison of the effects of continuous and intermittent electron irradiation on commercial 4H-SiC schottky barrier diodes, Nucl. Instrum. Methods Phys. Res. B 541 (2023) 355–362.
[21] N. Son, X. Trinh, L. Løvlie, B. Svensson, K. Kawahara, J. Suda, E. Janzén, Negative-U system of carbon vacancy in 4H-SiC, Phys. Rev. Lett. 109 (18) (2012) 187603.
[22] T. Dalibor, G. Pensl, H. Matsunami, T. Kimoto, W. Choyke, A. Schöner, N. Nordell, Deep defect centers in silicon Carbide monitored with deep level transient spectroscopy, Phys. Stat. Sol. A 162 (1) (1997) 199–225.
[23] G. Izzo, G. Litrico, L. Calcagno, G. Foti, F. La Via, Electrical properties of high energy ion irradiated 4H-SiC schottky diodes, J. Appl. Phys. 104 (9) (2008) 093711.
[24] S.M. Wang, R.B. Hu, G. Chen, C.T. Luo, M. Gong, Y. Li, Z.M. Yang, Investigation of 4H-SiC schottky barrier diodes irradiated with 6 MeV au ions at low temperature, Nucl. Instrum. Methods Phys. Res. B 494–495 (2021) 53–58.
[25] R. Singh, S. Arora, J. Singh, D. Kanjilal, In situ current-voltage characterization of swift heavy ion irradiated Au/n-GaAs schottky diode at low temperature, Radiat. Effect. Defect. Solid. 157 (4) (2002) 367–374.
[26] A. Kumar, A. Haehnel, D. Kanjilal, R. Singh, Electrical and microstructural analyses of 200 MeV Ag14+ ion irradiated Ni/GaN schottky barrier diode, Appl. Phys. Lett. 101 (15) (2012) 153508.
[27] A. Kumar, T. Kumar, A. Hähnel, D. Kanjilal, R. Singh, Dynamics of modification of Ni/n-GaN schottky barrier diodes irradiated at low temperature by 200 MeV Ag14 + ions, Appl. Phys. Lett. 104 (3) (2014) 33507.
[28] Johnson, A. Javanainen, A. Raman, P. Chakraborty, R. Arslanbekov, A. Witulski, J. Lauenstein, Unifying Concepts for Ion-Induced Leakage Current Degradation in Silicon Carbide Schottky Power Diodes. IEEE Trans. Nucl. Sci. 67 (1), 135–139 (2020).
[29] T. Knežević, A. Hadžipašić, T. Ohshima, T. Makino, I. Capan, M-center in low-energy electron irradiated 4H-SiC, Appl. Phys. Lett. 120 (25) (2022) 252101.
[30] Ł. Gelczuk, M. Dąbrowska-Szata, M. Sochacki, J. Szmidt, Characterization of deep electron traps in 4H-SiC junction Barrier schottky rectifiers, Solid-State Electron. 94 (2014) 56–60.
[31] T. Miyazaki, T. Makino, A. Takeyama, S. Onoda, T. Ohshima, Y. Tanaka, Y. Hijikata, Effect of gamma-ray irradiation on the device process-induced defects in 4H-SiC epilayers, Superlattices Microstruct. 99 (2016) 197–201.
[32] P. Klein, B. Shanabrook, S. Huh, A. Polyakov, M. Skowronski, J. Sumakeris, M. O'Loughlin, Lifetime-limiting defects in n-4H-SiC epilayers, Appl. Phys. Lett. 88 (5) (2006), 052110–052110-3.
[33] K. Danno, D. Nakamura, T. Kimoto, Investigation of carrier lifetime in 4H-SiC epilayers and lifetime control by electron irradiation, Appl. Phys. Lett. 90 (20) (2007) 202109.
[34] S. Tanimoto, Impact of dislocations on gate oxide in SiC MOS devices and high reliability ONO dielectrics, Mater. Sci. Forum 527–529 (2) (2006) 955–960.
[35] M. Grieb, D. Peters, A.J. Bauer, Influence of the oxidation temperature and atmosphere on the reliability of thick gate oxides on the 4H-SiC C(0001) face, Mater. Sci. Forum. 600–603 (2009) 597–602.
[36] S.T. Dunham, J.D. Plummer, Point-defect generation during oxidation of silicon in dry oxygen, I. Theory. J. Appl. Phys. 59 (7) (1986) 2541–2550.
[37] G. Alfieri, T. Kimoto, Resolving the EH6/7 level in 4H-SiC by Laplace-transform deep level transient spectroscopy, Appl. Phys. Lett. 102 (15) (2013) 152108.
[38] S. Tunhuma, F. Auret, H. Danga, J. Nel, M. Diale, In situ study of low-temperature irradiation-induced defects in silicon Carbide, J. Electron. Mater. 48 (6) (2019) 3849–3853.
[39] D. Davydov, A. Lebedev, V. Kozlovski, N. Savkina, A. Strel'chuk, DLTS study of defects in 6H- and 4H-SiC created by proton irradiation, Physica. b, Condensed Matter. 641–644 (2001) 308.
[40] M. Kozubal, P. Kamiński, R. Kozłowski, E. Tymicki, K. Grasza, S. Warchoł, Effect of electron irradiation on defect structure of 6H–SiC grown by PVT method, Superlattices Microstruct. 45 (4) (2009) 402–406.
[41] C.C. Ling, X.D. Chen, G. Brauer, W. Anwand, W. Skorupa, H.Y. Wang, H.M. Weng, Deep-level defects in n -type 6H silicon carbide induced by he implantation, J. Appl. Phys. 98 (4) (2005), 043508–043508-6.
[42] X.D. Chen, S. Fung, C.C. Ling, C.D. Beling, M. Gong, Deep level transient spectroscopic study of neutron-irradiated n-type 6H-SiC, J. Appl. Phys. 94 (5) (2003) 3004–3010.
[43] C. Hemmingsson, N. Son, O. Kordina, E. Janzén, J. Lindström, Capture cross sections of electron irradiation induced defects in 6H-SiC. J. Appl. Phys. 84 (2), 704-70 (1998)8.
[44] J. Racko, M. Mikolášek, P. Benko, O. Gallo, L. Harmatha, R. Granzner, F. Schwierz, Coupled defect level recombination in the P-N junction, J. Electr. Eng. 62 (6) (2011) 355–358.